Available online at www.sciencedirect.com
SCIENCE DIRECT®
Journal of Power Sources 158 (2006) 722–729
JOURNAL OF POWER SOURCES
www.elsevier.com/locate/jpowsour

The $Na_{0.60}CoO_2$ phase, a potential conductive additive for the positive electrode of Ni–MH cells

Frédéric Tronel [a,b], Liliane Guerlou-Demourgues [a,*], Maïté Basterreix [a], Claude Delmas [a]

[a] *Institut de Chimie de la Matière Condensée de Bordeaux-CNRS and Ecole Nationale Supérieure de Chimie et Physique de Bordeaux, Université Bordeaux I, 87 Av. Dr. A. Schweitzer, 33608 Pessac Cedex, France*
[b] *SAFT - Direction de la Recherche, 111-113 boulevard Alfred Daney, 33074 Bordeaux Cedex, France*

Received 9 March 2005; received in revised form 1 July 2005; accepted 22 July 2005
Available online 9 November 2005

Abstract

The $Na_{0.60}CoO_2$ phase, obtained by a classical solid-state reaction, is tested as a conductive additive in the nickel oxide electrode. Though the process was not optimised in terms of additive repartition, the experiments show a good efficiency of the $Na_{0.60}CoO_2$ phase even at low cobalt content, compared to usual additives like CoO. Moreover, it increases the stability of the electrode at low potential. The added $Na_{0.60}CoO_2$ phase is shown to transform, during the first cycles, into a γ-type cobalt oxyhydroxide phase that is more stable at low potential than the usual additives.

Keywords: Alkaline batteries; Sodium nickelate; Conductive additive

1. Introduction

When cobalt is co-precipitated within nickel hydroxide, the active material of the positive electrode of Ni–MH cells, it tends to increase the chargeability of the battery as well as the conductivity of the active material and to reduce the positive electrode swelling, thus improving the capacity and life duration of the battery [1–3]. When cobalt is post-added to nickel hydroxide, it plays a key role in the improvement of the performances of the non-sintered nickel hydroxide electrode. In such an electrode, low density nickel foam, with much larger pores than classical sintered substrate, plays both roles of substrate and current collector. Post-added cobalt forms a conductive network within the pores, which allows a full utilization of the active material [4,5] by linking electronically the active material (nickel hydroxide), located in the middle of the large pores, to the current collector. By this way, the use of cobalt conductive additive has allowed the manufacturing of high capacity nickel metal hydride batteries, now used in many portable devices.

The conductive network is formed during the beginning of the first charge of the electrode, from cobalt added under the form of CoO, $Co(OH)_2$ or cobalt salts [4]. The so-formed conductive phase, H_xCoO_2, is stable in the usual cycling potential range (approximately 0.9–1.5 V versus $Cd(OH)_2/Cd$) [6]. But this way of adding cobalt exhibits some drawbacks. When held at low potential, which could occur during a deep discharge of the cell or a storage in a discharge state, the cobalt conductive phase is likely to be reduced into $Co(OH)_2$. According to Pralong et al., this reaction takes place at 0.67 V versus $Cd(OH)_2/Cd$ [7]. The $Co(OH)_2$ phase is soluble, so that the cobalt derivatives tend to migrate into the electrode or to be redeposited as insulating phases like stoichiometric CoOOH or Co_3O_4 [8,9]. Actually, this results in a decrease in the efficiency of the cobalt conductive network.

Research groups and battery manufacturers have proposed new processes and new additives to overcome these drawbacks. Conductive "Co_3O_4" type spinel phases were thus prepared in specific conditions in our laboratories. The structure and the physical properties of these derivatives will be reported in a forthcoming paper [10]. Other conducting materials recently proposed are γ-type cobalt oxyhydroxide phases, which are hydrated derivatives of H_xCoO_2 with a higher oxidation state for cobalt, or Na containing cobalt phases [6,11–13]. All these materials are conductive and contain cobalt at a high oxidation

* Corresponding author. Tel.: +33 5 4000 2725; fax: +33 5 4000 6698.
E-mail address: guerlou@icmcb-bordeaux.cnrs.fr (L. Guerlou-Demourgues).

0378-7753/$ – see front matter © 2005 Elsevier B.V. All rights reserved.
doi:10.1016/j.jpowsour.2005.07.091

state (Co^{3+} and Co^{4+}). But these works are more focused on the efficiency of the thus manufactured cells than on the chemistry of the involved materials.

The following work aims at studying the potentialities of the $Na_{0.60}CoO_2$ phase as conductive additive. This phase, which was first synthesised by Fouassier et al. [14] in the 70 s, exhibits like H_xCoO_2 a lamellar structure based on stacked CoO_2 slabs. Cobalt in $Na_{0.60}CoO_2$ has an overage oxidation state of 3.4 and the phase exhibits metallic properties [15]. This material is therefore a good candidate as conductive additive. The present paper describes the electrochemical and chemical behaviour of the $Na_{0.60}CoO_2$ phase, as additive in the nickel oxide electrode. In order to understand the processes involved, this study was extended to the behaviour of pure $Na_{0.60}CoO_2$ electrodes in alkaline batteries.

2. Experimental

X-ray diffraction (XRD) patterns were collected with a Siemens D5000 diffractometer (Cu Kα). They were recorded with a scan step of 0.02° (2θ) for 10 s for the pristine material powder and of 0.06° (2θ) for 4 s for the electrode materials.

Electrochemical tests were performed in galvanostatic and potentiostatic modes. Galvanostatic experiments were processed with a homemade cycling apparatus in order to test the effect of additive upon the nickel oxide electrode. Potentiostatic experiments were processed on a Macpile (Biologic) device upon electrodes containing only cobalt phases. The recorded potentials are given versus $Cd(OH)_2$/Cd electrochemical couple. Charge and discharge rates are given as *C*/*n*, meaning than 1 electron is exchanged per nickel or cobalt in *n* hours.

3. The $Na_{0.60}CoO_2$ phase

3.1. Synthesis process

The $Na_{0.60}CoO_2$ phase was prepared by solid-state reaction from Co_3O_4 and Na_2O (Aldrich 99% min, 12% excess), in a tubular furnace at 550 °C during 15 h under flowing O_2 [14]. The Co_3O_4 starting material was previously obtained by decomposition of $CoCO_3$ (Fluka 99%) at 400 °C for 12 h under flowing O_2.

3.2. XRD study

The XRD pattern of the obtained phase is presented in Fig. 1. No significant impurity phase is observed. This phase crystallizes in the trigonal system (space group *R*3*m*) with a P3 oxygen stacking, usual in lamellar phases. The pattern is indexed with a hexagonal cell. The corresponding cell parameters are $a = 2.825$ Å and $c = 16.532$ Å, in good agreement with crystallographic data obtained by Fouassier et al. [14]. The interslab distance is therefore equal to 5.511 Å. More rigorously, the phase should be indexed in the monoclinic system as it exhibits a slight monoclinic distortion (P′3 oxygen stacking instead of P3), which can be seen as an example with the $(015)_{hex.}$ diffraction line exhibiting a noticeable shoulder at low angle. As the distortion is very weak, it was not considered in this work.

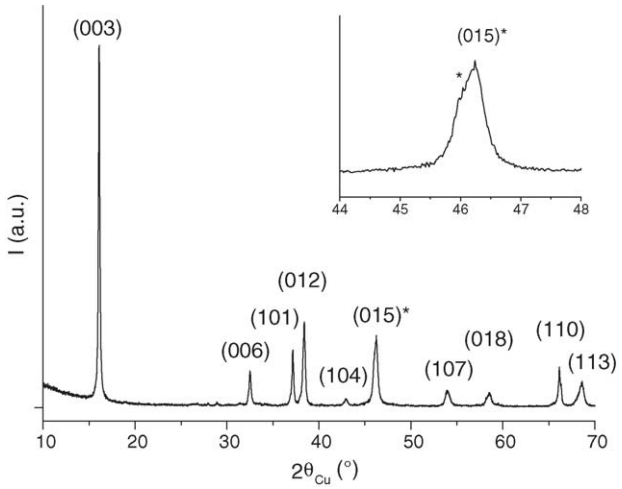

Fig. 1. XRD pattern of the synthesised $Na_{0.60}CoO_2$ phase (indexed with an hexagonal cell). Zoom of the $(015)_{hex.}$ diffraction line showing the slight monoclinic distortion.

3.3. Chemical composition

The cobalt content in the sample was measured by EDTA complexometric titration in an acidic buffer medium with xylenol orange tetrasodium salt as indicator. The sodium amount was determined by atomic emission spectrometry at 370.8 nm using a Perkin-Elmer 2280 apparatus. For both previous measurements, the powders were dissolved by heating in pure hydrochloric acid. The oxidation state of cobalt was measured by iodometric titration. For such measurements, the samples were dissolved by a reducing KI–HCl solution in an airtight container at 60 °C in order to prevent iodine evaporation.

The titration results are presented in Table 1 together with the values calculated on the basis of the $Na_{0.60}CoO_2$ ideal formula. Cobalt and sodium contents are slightly lower than expected. The Na/Co ratio of 0.60 and the value of 3.4 for cobalt oxidation state correspond to the expected values. The difference in sodium and cobalt contents could mean that the phase, which is stored in air, has adsorbed some water.

3.4. Electric properties

Around 200 mg of the obtained material were pressed (3 t cm^{-2}) into 8 mm diameter pellets. Conductivity measure-

Table 1
Weight percentages, molar ratios and average cobalt oxidation state for the $Na_{0.60}CoO_2$ phase, compared to the theoretical values calculated on the basis of the ideal formula

	Cobalt (wt.%)	Sodium (wt.%)	Na/Co (molar ratio)	Average oxidation state of cobalt
Ideal $Na_{0.60}CoO_2$	56.27	13.16	0.60	3.40
$Na_{0.60}CoO_2$ (studied)	54.0	12.6	0.60	3.4

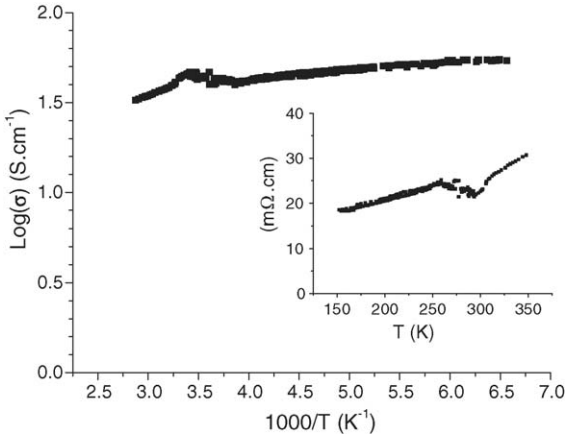

Fig. 2. Variation of logarithm of electrical conductivity vs. reciprocal temperature for the $Na_{0.60}CoO_2$ phase. The variation of the resistivity vs. T is in insert.

ments were performed between 150 and 350 K using a four probe technique [16].

Conductivity logarithm versus reciprocal temperature is displayed in Fig. 2. The value (around 40 S cm^{-1}) at room temperature is rather high. Moreover, the decrease of conductivity with increasing temperature shows the metallic behaviour of this phase. This behaviour results from a delocalisation of electrons within the cobalt slab due to the presence of at least 30% of tetravalent cobalt and to the small Co–Co distance. In this edge-sharing octahedron structure, the t_2–t_2 orbital overlapping through edges allows the formation of a metallic t_2 band when the Co–Co distance is smaller than a critical value, determined by Goodenough's formula. In the present case, $d_{Co–Co} = 2.825$ Å an $R_c = 2.885$ Å. Such conductivity values make the $Na_{0.60}CoO_2$ phase, a suitable candidate as a conductive additive for nickel hydroxide electrodes.

4. Use of $Na_{0.60}CoO_2$ as additive in the nickel oxide electrode (NOE)

4.1. Effect on the nickel utilization rate

4.1.1. Preparation of the electrodes and cycling conditions

In order to prepare electrodes for the electrochemical tests, the Na_xCoO_2 phase was mixed in two different proportions (33 or 10 wt.%) to "industrial" spherical nickel hydroxide. One weight percent PTFE was added as mechanical binder. Approximately 200 mg of the mixture were then pasted onto a piece of nickel foam (1 cm × 5 cm). The so-formed electrode was pressed at 1 t cm^{-2}, wrapped in a polypropylene separator and placed between two over-capacitive sintered cadmium electrodes (approximately 20 times the capacity of the positive electrode), which play both roles of reference and counter-electrodes. Similar cells, either without any additive or with 10 wt.% of CoO as conductive additive in the positive electrodes instead of Na_xCoO_2, were used for comparison. A 8 M KOH solution was used as electrolyte. The theoretical capacity of one electrode, based on one electron discharged per nickel atom, was in the 50–70 mAh range depending on the amount of additive.

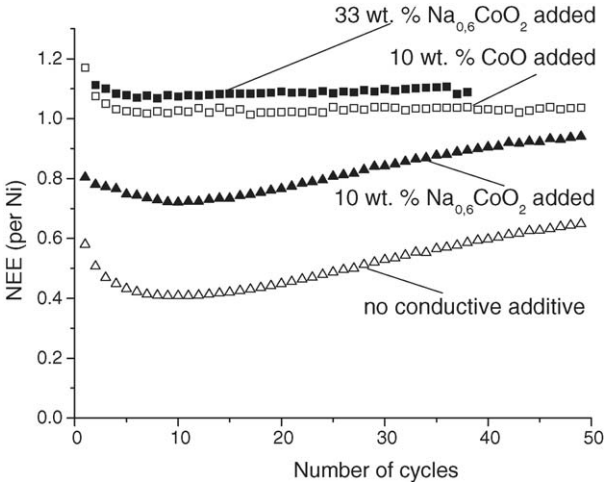

Fig. 3. Evolution of the number of exchanged electrons (NEE) per nickel atom during a galvanostatic cycling at the *C*/5 rate in 8 M KOH for nickel electrodes containing 33 or 10 wt.% of $Na_{0.60}CoO_2$ as conductive additive. The NEE for electrodes containing 10 wt.% CoO or no additive are presented for comparison.

The cycling of the cells begins with a 20 h charge at the *C*/10 rate, followed by cycles including a discharge at *C*/5 with a cut-off voltage of 0.9 V and a 6 h charge at *C*/5.

In the following, the capacity is given by the number of exchanged electrons (NEE) per nickel atom during the discharge. By this way, the efficiency of the additive to improve utilization of nickel hydroxide is easy to follow.

4.1.2. Results and discussion

The evolution of the NEE for 10 and 33 wt.% of $Na_{0.60}CoO_2$ are presented in Fig. 3, and compared to the evolution of the NEE for the reference cells using either 10 wt.% CoO as conductive additive or no additive. The value of the NEE for the electrode containing 33 wt.% $Na_{0.60}CoO_2$ is stable around 1.1 electron per nickel atom, which has to be compared to 1.05 electron for the reference electrode containing CoO and in the 0.4–0.7 electron range without additive. With 10 wt.% $Na_{0.60}CoO_2$, the starting capacity is much lower (around 0.7–0.8 exchanged electron). But the NEE, after a significant decrease (around 0.1 electron) during the first 10 cycles, is increasing regularly and stabilizes at 0.9 electron exchanged around the 50th cycle. NEE values for the various electrodes at the 35th and at 50th cycles are gathered in Table 2. These results show that the addition of $Na_{0.60}CoO_2$,

Table 2
Number of exchanged electrons (NEE) values per Ni atom for nickel oxide electrodes using different conductive additives: no additive, 10 wt.% CoO, 10 wt.% $Na_{0.60}CoO_2$ and 33 wt.% $Na_{0.60}CoO_2$

Electrode	NEE per nickel atom (35th/50th cycle)	Capacity of the pasted material (mAh g^{-1}) (35th/50th cycle)
Without additive	0.56/0.65	149/173
10 wt.% CoO	1.04/1.04	249/249
10 wt.% $Na_{0.6}CoO_2$	0.78/0.94	208/223
33 wt.% $Na_{0.6}CoO_2$	1.1/–	193/–

The resulting capacities (in mAh g^{-1}) for the pasted materials are also displayed.

whatever the amount, leads to a significant increase in the utilization of nickel hydroxide, even not as good as with CoO for the same weight amount.

The latter results are presenting the effect of the additive by considering the NEE per nickel atom, but from a practical viewpoint, the global efficiency of the pasted material should be considered, the aim being high specific capacities. The specific capacities of the different pasted materials in mAh g^{-1} are thus displayed in Table 2, even if it is clear that an electrode with 33 wt.% of additive is only for laboratory purpose. From that point of view, the pasted material with 10 wt.% CoO has the higher capacity (249 mAh g^{-1}) and the material containing 33 wt.% $Na_{0.60}CoO_2$, despite a high NEE per nickel atom, exhibits a rather poor weight capacity. The pasted material with 10 wt.% $Na_{0.60}CoO_2$ has a relatively good capacity though not as good as that obtained with CoO. Nevertheless, it should be noticed that the studied material is far from being optimised. As reported in the synthesis section, the $Na_{0.60}CoO_2$ phase used in the experiments has indeed been obtained by a solid-state reaction, which, despite a rather moderate process temperature (550 °C), is used to lead to relatively large particles. For a conductive additive, whose ability to spread all over the electrode is a key property, large particles are a main drawback. The necessary amount of conductive additive will indeed be higher in the case of large particles than in the case of small ones [17].

From a practical point of view, the use of $Na_{0.60}CoO_2$ exhibits another attractive characteristics. Actually, the wt.% of cobalt added should be considered instead of the percentage of additive ($Na_{0.60}CoO_2$ or CoO), which includes oxygen and sodium, because the price of the additive is closely linked to the amount of cobalt. In our case, 10 wt.% of $Na_{0.60}CoO_2$ corresponds to 5.62% of cobalt (metal), 10% of CoO to 7.86% of cobalt and 33% of $Na_{0.60}CoO_2$ to 18.75% of cobalt.

In the case of 10 wt.% $Na_{0.60}CoO_2$ added, it should also be mentioned that the capacity was much more varying depending on the experiments than with 33 wt.%. Close to the minimum amount of additive allowing percolation of the cobalt conductive network into the electrode, important variations in capacity for different experiments are expected. Ten weight percent of $Na_{0.60}CoO_2$ should thus be close to that limit. Concerning the significant increase of the capacity of such electrodes, this activation phenomenon, as also occurring for electrodes without additive, is probably linked for a major part to cycling conditions, which involve a strong overcharge at each cycle, resulting from the low utilization rate of $Ni(OH)_2$ in the previous discharge (70% overcharge if NEE = 0.7 and 100% if NEE = 0.6). But, in this preliminary study, only two additive amounts were considered. A more general study is in progress.

4.2. Improved stability of the electrode

4.2.1. Testing procedure for low potential storage

A key test, for practical purpose, of Ni–Cd and Ni–MH cells is the low potential storage [11]. Actually a classical NOE using CoO or $Co(OH)_2$ as conductive additive undergoes a significant capacity loss when stored days long in short-circuit. As already mentioned in Section 1, various papers have shown that such decrease was due to the reduction of the conductive H_xCoO_2 phase into $Co(OH)_2$ and, as a result of the solubility of this latter phase in the electrolyte, a migration of cobalt species in the electrode, leading to a reduced efficiency of the cobalt conductive network [7,18]. The classical way to test resistance of a cell towards such effect is to leave it after discharge during some days shorted on a resistor. In the present case, electrodes made with 10, 33% $Na_{0.60}CoO_2$ or 10% CoO are cycled during approximately 50 cycles, then shorted for 3 days on a 10 Ω resistor. Some cycles are performed in the initial conditions after this storage in order to measure the remaining capacity of the electrode.

4.2.2. Results and discussion

The evolutions of the NEE of the studied electrodes versus the number of cycles are presented in Fig. 4. While the reference electrode, with CoO as additive, undergoes a 12% loss of its capacity after storage, the electrode with 33% $Na_{0.60}CoO_2$ does not suffer from any significant loss of capacity. More surprisingly, the electrode with 10% $Na_{0.60}CoO_2$ added shows an increase of 8% of its capacity after storage, leading to a capacity as good as with CoO. It should be mentioned that if only one experiment is presented in Fig. 4, many similar results have been obtained.

These experiments show that $Na_{0.60}CoO_2$ prevents from the mechanism leading to a degradation of the cobalt conductive network. This mechanism was supposed to occur via a step of reduction of the cobalt conductive phase and a dissolution-re-precipitation step [7,8,18], but with the present results it is not possible to choose which step is affected. Concerning the increase of the capacity in the case of 10% $Na_{0.60}CoO_2$ added, it could be addressed to an improvement of the repartition of the conductive phase within the electrode at low potential, but such mechanism would implicate a migration of cobalt via the solution, which is not compatible with the stability of highly oxidized phases, cobalt being at the oxidation state of 2 in solu-

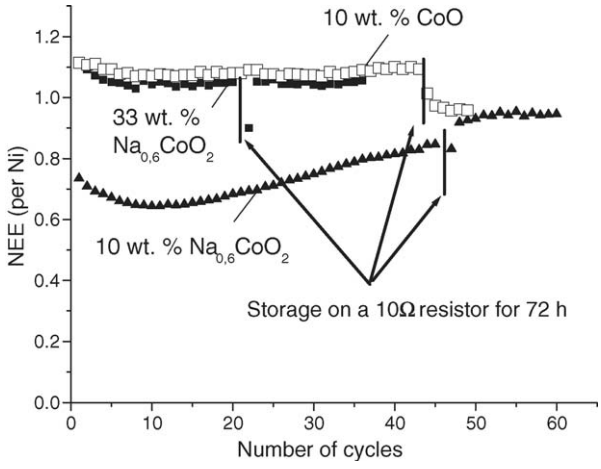

Fig. 4. Evolution of the number of exchanged electrons (NEE) per nickel atom during the galvanostatic cycling at the *C*/5 rate in 8 M KOH and subjected to a low potential storage (shorted on a resistor) for nickel electrodes using 33 or 10 wt.% of $Na_{0.60}CoO_2$ or 10 wt.% CoO as conductive additive.

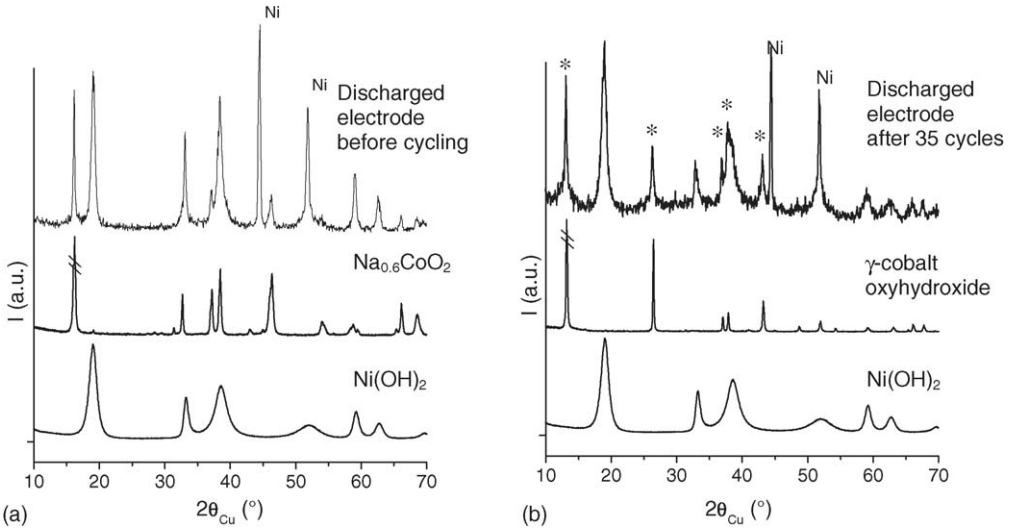

Fig. 5. XRD patterns of discharged nickel electrodes using 33 wt.% of $Na_{0.60}CoO_2$ as conductive additive (a) before cycling and (b) after 35 cycles. Reference patterns of the $Ni(OH)_2$ phase, of the starting $Na_{0.60}CoO_2$ phase and of the γ-type cobalt oxyhydroxide phase are also shown. ((*) Peaks corresponding to the γ-phase in the pattern of the cycled electrode).

tion [19]. Further experiments are in course to understand this phenomenon.

5. Chemical and electrochemical behaviour of the $Na_{0.60}CoO_2$ phase used as electrode material

More attention will now be focused on the behaviour of the $Na_{0.60}CoO_2$ phase as electrode material in order to understand the positive effect of such compound.

5.1. Evolution within the nickel hydroxide electrode

The electrodes containing 33 wt.% of $Na_{0.60}CoO_2$ were investigated by XRD before cycling and after 40 cycles, in the discharge state. The XRD patterns are presented in Fig. 5a and b. Reference patterns of $Ni(OH)_2$, $Na_{0.60}CoO_2$ and a γ-Co oxyhydroxide phase are also displayed for comparison. This γ-Co oxyhydroxide was synthesised by oxidative hydrolysis of the $Na_{0.60}CoO_2$ phase in a NaClO/KOH (1:5) solution, using the process described by Butel et al. [6].

In the case of the starting electrode (Fig. 5a), as expected, the diffraction lines of the $Na_{0.60}CoO_2$ phase are observed together with those corresponding to $Ni(OH)_2$. After cycling (Fig. 5b), no diffraction line characteristic of $Na_{0.60}CoO_2$ can be seen any more; in particular the (0 0 3) line at $2\theta_{Cu} = 16.1^\circ$ has disappeared. Besides, five narrow diffraction lines can be observed, corresponding to a γ-type oxyhydroxide, that could a priori be nickel or cobalt oxyhydroxide from a strictly structural point of view. But it has been usually observed that the γ-Ni phase, which could be seen in electrodes even in a discharge state, exhibits very broad peaks especially after several cycles [20]. The narrow peaks observed in the present work should then correspond to a γ-Co oxyhydroxide phase. Such result is not surprising because γ-Co oxyhydroxide can be obtained by chemical oxidizing hydrolysis (in a NaClO/KOH mixture) from $Na_{0.60}CoO_2$ [6]. A similar process could occur during the charge of the electrode.

5.2. Voltammetric study of $Na_{0.60}CoO_2$

5.2.1. Cyclic voltammetry of the $Na_{0.60}CoO_2$ phase

Pasted electrodes, containing only $Na_{0.60}CoO_2$ as active material, were manufactured by the same process as for nickel oxide electrodes, with only 1 wt.% of PTFE added as mechanical binder. A cyclic voltammetry experiment was performed on these electrodes using a Macpile potentiostatic controller (Biologic). A $Cd(OH)_2$/Cd electrode was used as counter and reference electrode. The scan rate was 2.5 mV min^{-1} with 2.5 mV potential steps. The potential window was chosen in the 0.5–1.5 V range, which allows to scan the usual cycling window (0.9–1.5 V) as well as the 0.5–0.9 V potential window, where reduction of Co^{3+} ions is likely to occur. The evolutions of the average intensity during a potential step versus potential for the first five discharges and charges of a $Na_{0.60}CoO_2$ electrode are presented in Fig. 6.

The voltammogram is continuously modified during the very first cycles, then a steady state is obtained after the fifth cycle. During the first oxidation, no electrochemical activity is measured until 1.12 V, where a first oxidation peak takes place; a second peak appears at 1.39 V. In the following cycles, three peaks are noticeable in oxidation as well as in reduction. The electrochemical phenomena occur at 1.01, 1.09 and 1.39 V in oxidation and 1.17, 0.93 and 0.88 V in reduction. One additional small and wide reduction peak can be observed only in the first cycle at 1.32 V. Above 1.45 V, the intensity increase is only due to irreversible electrolyte oxidation into oxygen (oxygen evolution reaction: OER). Actually, this phenomenon is likely to begin at a lower potential but with a lower kinetic. As a consequence, even when the potential is decreasing, an oxidation peak can be sometimes observed over 1.4 V (see also Fig. 8b). When com-

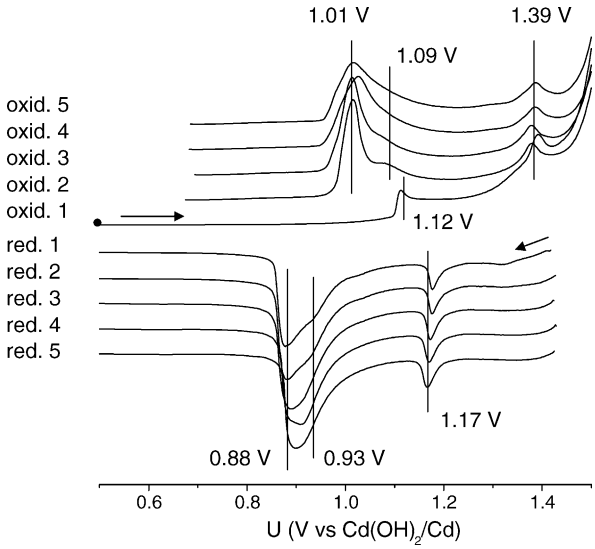

Fig. 6. Evolution of intensity vs. potential during the first 5 voltammetric cycles of an electrode whose active starting material is the $Na_{0.60}CoO_2$ phase.

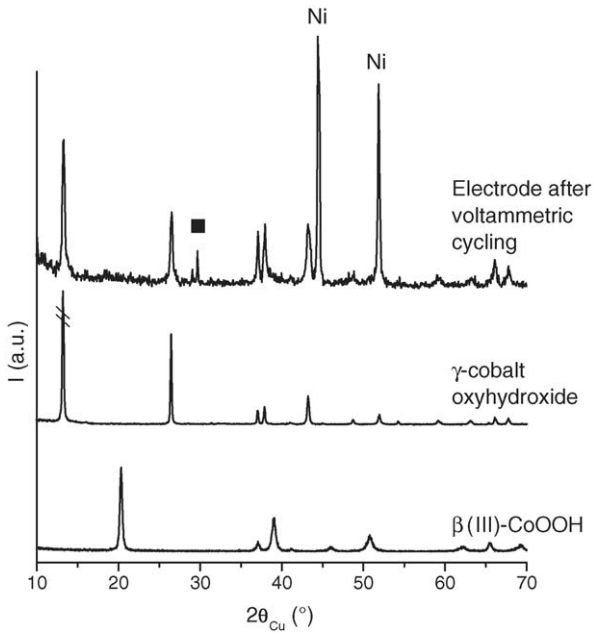

Fig. 7. XRD patterns of an electrode whose active starting material is the $Na_{0.60}CoO_2$ phase after 5 cycles of voltammetric cycling. Reference patterns of the γ-type cobalt oxyhydroxide phase and of the β(III) type CoOOH are also shown. ((■) Diffraction lines assigned to crystallized KOH or carbonate).

paring the various oxidation curves, it clearly seems that the first peak at 1.12 V concerns the same phenomenon as the 1.09 V in the subsequent cycles. Besides, the two most important oxidation peaks at 1.01 and 1.09 V combine in the first cycles to form a wide asymmetric peak in oxidation 5. A similar phenomenon occurs with the 0.88 and 0.93 V reduction peaks, which form a wide asymmetric peak at 0.9 V in reduction 5. It is likely to suggest that these reduction peaks (0.88 and 0.93 V) corresponds to the same electrochemical reactions (though in reduction) than the previous oxidation peak (1.01 and 1.09 V).

Considering that the starting material contains only Co^{3+} and Co^{4+} and that the capacity reversibly exchanged in a charge–discharge process never exceeds 0.1 electron per cobalt atom, the cycling probably occurs only between these two cobalt oxidation states (3+ and 4+). But it has not been possible to link the peaks to specific electrochemical phenomena. Besides, no significant redox phenomenon occurs in the 0.5–0.85 V potential range. As this latter behaviour could be accounted to the reduction at low potential of the conductive phase into an insulating one, that would prevent any further electrochemical activity of the material in the low potential range, similar experiments with 33 wt.% of graphite added to electrode composition were performed (not presented), confirming the absence of any electrochemical activity at low potential. Actually, some authors have shown that, in cycling conditions, the oxidized cobalt phases, such as H_xCoO_2 or γ-Co oxyhydroxide are irreversibly reduced into the $HCoO_2$ phase, which is further reduced at 0.67 V, leading to soluble Co^{2+} responsible for degradation of the cobalt conductive network [17,18]. From that point of view the $Na_{0.60}CoO_2$ phase seems to be more stable, since no significant reduction peak appears in that potential range.

The XRD pattern of an electrode, recovered after the fifth discharge, is presented in Fig. 7. The observation of the XRD pattern thus confirms unambiguously the observation of Fig. 5: no diffraction line of $Na_{0.60}CoO_2$ is observable and the pattern corresponds to a γ-Co oxyhydroxide, whose XRD pattern is presented as reference. Concerning the possibility for highly oxidized cobalt phases to be reduced in $HCoO_2$, no peak corresponding to this phase, whose XRD pattern is also displayed, can be observed.

5.2.2. *Low potential domain*

To look more precisely to the low potential zone in usual cycling conditions, a specific cycling program was performed upon a similar $Na_{0.60}CoO_2$ electrode. Five cycles of oxidation–reduction at 2.5 mV min^{-1} between 0.9 and 1.5 V were processed to reproduce a classical cycling. Then the potential was decreased by steps of 2.5 mV down to 0.2 V. The change to the next potential step is imposed as soon as the current has decreased down to a value corresponding to a *C*/450 rate. Such conditions ensured that no significant electrochemical process is occurring when the next potential step begins. In this experiment, the electrode remains below 0.5 V for 4 h. Five additional cycles between 0.9 and 1.5 V are then performed, identically to the first five cycles, in order to look for differences. The evolutions of intensity versus potential are displayed in Fig. 8a for all charges, Fig. 8b for all discharges. The variation of potential versus number of exchanged electrons for the low potential discharge is presented in Fig. 8c.

During the first five cycles (Fig. 8a and b) the evolution is globally identical to that observed in Fig. 6, but slower, probably because of the higher reduction cut-off voltage (0.9 instead of 0.5 V). Note that, between the end of the fifth discharge (down to 0.9 V) and the beginning of the reduction scan down to 0.2 V, a short relaxation period has taken place, leading to slight reincrease of the potential up to 0.97 V. During the reduction scan of the electrode from 0.9 down to 0.2 V, approximately 0.025 elec-

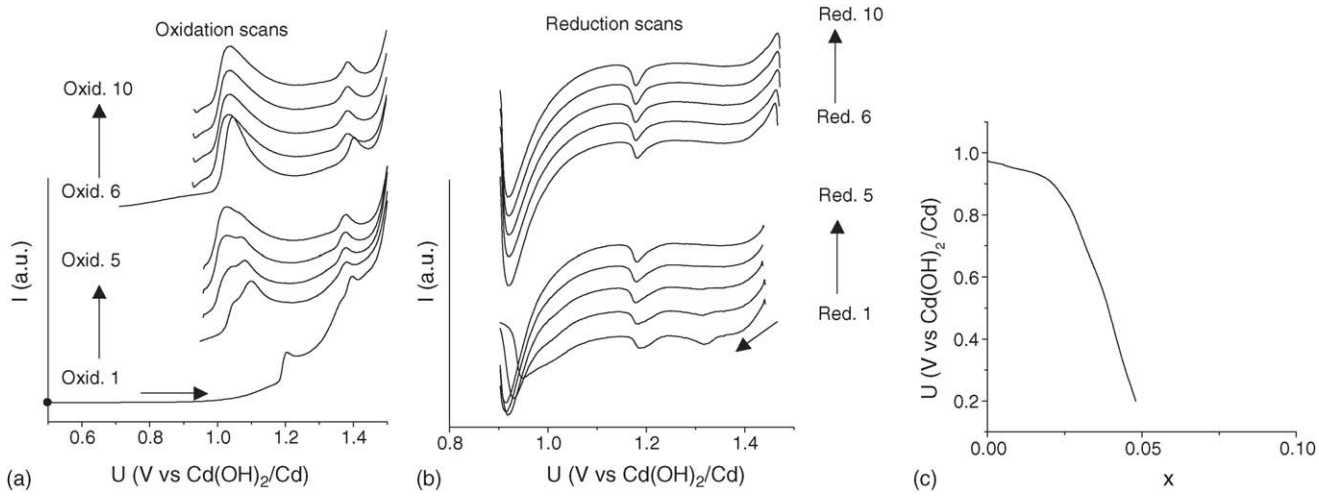

Fig. 8. Evolution of intensity vs. potential during the 10 cycles of voltammetric cycling of an electrode pasted with the $Na_{0.60}CoO_2$ phase, with a deep reduction down to 0.2 V between cycle 5 and 6: (a) in oxidation, (b) in reduction and (c) variation of the potential vs. the molar ratio x of injected electrons in the electrode during reduction down to 0.2 V after the fifth voltammetric reduction.

tron per cobalt is discharged between 0.9 and 0.2 V (Fig. 8c) and no plateau corresponding to a significant reduction reaction is observed, in accordance with the results of the previous part, that show no significant electrochemical activity in reduction in the 0.9–0.5 V range. Moreover, the voltammogram after this reduction scan (Fig. 8a and b) has a shape similar to that observed before. The studied material has thus not been transformed, at least from an electrochemical point of view, by the low potential reduction.

5.3. Discussion

In electrochemical cycling conditions, the $Na_{0.60}CoO_2$ phase transforms into a γ-Co oxyhydroxide phase, which is known as so good a conductor as the pristine phase [6]. The so formed phase cannot be reduced at low potential and does not transform into $HCoO_2$, which is usually responsible for the damage of the conductive network. These results seem in contradiction with those previously obtained by Butel about γ-Co oxyhydroxide, which showed a progressive transformation of this phase into $HCoO_2$ during cycling [17]. In this latter work, the γ-Co oxyhydroxide, which contained a very small amount of remaining sodium, was tested. The presence of sodium in the starting material, in our case, could possibly address the differences in stability. Additional in situ cycling experiments are in course to clear this point.

6. Conclusion

$Na_{0.60}CoO_2$ phase was shown to be a good conductive additive for the positive electrode of nickel–metal hydride or nickel–cadmium cells. When post-added within the nickel oxide electrode, it leads to a good capacity for the electrode, though slightly lower than when CoO is post-added. Moreover, the use of $Na_{0.60}CoO_2$ improves the capacity recovery of the cell after storage at low potential.

The active cobalt phase within the electrode was shown to be a γ-type cobalt oxyhydroxide, in which the $Na_{0.60}CoO_2$ phase transforms during the first cycles. The improved stability at low potential of electrodes, using $Na_{0.60}CoO_2$ as conductive additive, is probably linked to the fact that this γ-type phase cannot be reduced at low potential.

Additive experiments are in course in order to answer the remaining questions upon the structure of the formed phases and the possible role of sodium towards the stability of the γ-type phase in discharge.

Acknowledgements

The authors thank R. Decourt for electric properties measurements, C. Denage for technical assistance, Saft, ANRT and Region Aquitaine for financial support.

References

[1] P. Oliva, J. Leonardi, J.F. Laurent, C. Delmas, J.J. Braconnier, M. Figlarz, F. Fievet, A. De Guibert, J. Power Sources 8 (1982) 229.
[2] A. Cressent, V. Pralong, A. Audemer, J.B. Leriche, A. Delahaye-Vidal, J.M. Tarascon, Solid State Sci. 3 (2001) 65.
[3] M. Oshitani, T. Takayama, K. Takashima, S. Tsuji, J. Appl. Electrochem. 16 (1986) 403.
[4] M. Oshitani, H. Yufu, K. Takashima, S. Tsuji, Y. Matsumaru, J. Electrochem. Soc. 136 (1989) 1590.
[5] M. Oshitani, M. Watada, T. Tanaka, T. Iida, The Electrochemical Society Proceedings Series, vol. 94-27, 1994, p. 303.
[6] M. Butel, L. Gautier, C. Delmas, Solid State Ionics 122 (1999) 271.
[7] V. Pralong, A. Delahaye-Vidal, B. Beaudoin, J.B. Leriche, J.M. Tarascon, J. Electrochem. Soc. 147 (2000) 1306.
[8] A.H. Zimmerman, R. Seaver, J. Electrochem. Soc. 137 (1990) 2662.
[9] V. Pralong, A. Delahaye-Vidal, B. Beaudoin, J.B. Leriche, J. Scoyer, J.M. Tarascon, J. Electrochem. Soc. 147 (2000) 2096.
[10] F. Tronel, L. Guerlou-Demourgues, M. Ménétrier, L. Croguennec, L. Goubault, P. Bernard, C. Delmas, in preparation.
[11] Matsushita, European Patent, EP 0851 516 A2 (1998).

[12] Sanyo, European Patent, EP 0757 395 A1 (1997).
[13] Tanaka, Japanese Patent, JP 2001–52695 (2001).
[14] C. Fouassier, G. Matejka, J.M. Reau, P. Hagenmuller, J. Solid State Chem. 6 (1973) 532.
[15] C. Fouassier, C. Delmas, P. Hagenmuller, Mat. Res. Bull. 10 (1975) 443.
[16] J. Laplume, L'onde électrique 335 (1955) 113.
[17] M. Butel, Thesis of University Bordeaux I, 1998.
[18] V. Pralong, A. Delahaye-Vidal, Y. Chabre, B. Beaudoin, J.M. Tarascon, J. Solid State Chem. 162 (2001) 270.
[19] M. Pourbaix, Atlas d'équilibres électrochimiques, Gauthier Villars Paris ed., 1963, p. 342.
[20] C. Tessier, C. Faure, L. Guerlou-Demourgues, C. Denage, G. Nabias, C. Delmas, J. Electrochem. Soc. 149 (2002).